



Retrieval of refractive index and water content for the coating materials of aged black carbon aerosol based on optical properties: a theoretical analysis

Jia Liu^{a,b,c}, Cancan Zhu^{a,b,c}, Donghui Zhou^{a,b,c}, Jinbao Han^{a,b,c}

5 ^a Non-destructive Testing Laboratory, School of Quality and Technical Supervision, Hebei University, Baoding 071002, China.

^b Engineering Research Center of Zero-carbon Energy Buildings and Measurement Techniques, Ministry of Education, Hebei University, Baoding 071002, China.

^c Hebei Key Laboratory of Energy Metering and Safety Testing Technology, Hebei University, Baoding 071002, China.

10 Correspondence to: Jia Liu (liujia@hbu.edu.cn)

Abstract. Water content in the coatings of aged black carbon (BC) aerosol can be reflected through complex refractive index. In this study, the retrieval of refractive index and water content for the non-absorbing coatings of BC aerosol during the hygroscopic growth (RH=0-95%) based on scattering and absorption properties is theoretically investigated. Optical properties of morphologically realistic fractal BC aerosols are simulated using the Multiple Sphere *T*-matrix method (MSTM), the optical equivalent refractive index of coating material is retrieved based on the Mie theory, and the water content in coatings is further retrieved using effective medium theory. Results show that the scattering property has the best performance in retrieving refractive index and water content. The retrieval errors of the refractive index of heavily-aged BC aerosols are less than 10% at high RHs, while partially-coated and thinly-coated BC have larger errors. The retrieved water contents are similar to those of refractive index and the errors range from 2% to 63% for heavily-coated BC. This study provides a helpful optical method to obtain the water content of BC coatings.

1 Introduction

Black carbon (BC) aerosols are ubiquitous in the Earth's atmosphere and directly lead to global and regional warming by scattering and absorbing solar radiation (Zhang et al., 2019b; Zhang et al., 2020). Since BC is mainly produced by incomplete combustion of fossil fuel and biomass, various microphysical characteristics determine the diversity of scattering and absorption properties, which further bring huge uncertainty in the radiative and climate effects of BC (Zhang et al., 2019a). Fresh bare BC will be coated by inorganic salts or organics during aging process such as condensation and collision in the atmosphere, and hydrophobic BC aerosol becomes hydrophilic. The optical properties of coated BC may be significantly different from the bare one and enlarge the uncertainty of radiative effect, not only because of the morphology



30 change of fractal structure but also due to the “lensing effect” or “sunglass effect” caused by coating materials with different complex refractive indices (Luo et al., 2018b). Therefore, the determination of complex refractive indices (CRIs) of coated BC and even only the coating material is essential for field and laboratory observations.

Refractive index of aerosols, $m=n+ki$, can be determined from the scattering and absorption properties, the real part is related to the former and the imaginary part is related to the latter. With the assistance of a self-developed cavity-enhanced
35 albedometer, (Zhao et al., 2014; Xu et al., 2016) measured the extinction coefficient, scattering coefficient, absorption coefficient and single scattering albedo (SSA) for atmospheric aerosols at Jing-Jin-Ji Area, effective CRIs of aerosols were retrieved based on Mie theory of homogeneous sphere using measured optical properties and the well-known volume mixing role, that is the effective CRI is the volume-weighted average (VWA) of each aerosol component, the retrieved real part and
40 imaginary part of CRIs were about 1.38-1.44 and 0.008-0.04 respectively. Zhao et al. (2019) combined a differential mobility analyzer (DMA) and a single-particle soot photometer (SP2) to characterize the scattering properties of size-resolved ambient aerosol at a suburban site, the real part of CRIs retrieved using Mie calculation was 1.34-1.56 and increase slowly with the aerosol diameter. At four different sites in China, Zhao et al. (2021) revealed that the real part of CRIs ranged from 1.36 to 1.78 and increased with the mass ratio of organics. Radney and Zangmeister (2018) compared two aerosol CRI retrieval methods based on Mie scattering theory, the first method employed measurements of optical properties
45 of size-selected particles while the second method employed measurements of both optical properties and particle size distributions, they recommended the application of these methods in laboratory and field observations respectively. Through the combination of a novel broadband cavity enhanced spectroscopy and a DMA, the aging process of pinene and xylene and the production of secondary organic aerosols (SOA) in an oxidation flow reactor were investigated by He et al. (2018), extinction properties were used to retrieve CRIs, results showed that SOAs are not absorbing in visible range while the real
50 part of CRIs depends slightly on wavelength. With special attention to coatings of BC, Xu et al. (2018) investigated the optical properties of aerosols in field observations using an albedometer, based on core-shell Mie theory for coated BC, the imaginary part of CRIs was retrieved to be 0.004-0.008. Through an instrument setup consisting of aethalometer, nephelometer, aerodynamic particle sizer (APS), DMA, and SP2, Zhao et al. (2020) measured absorption coefficient, scattering coefficient, size distribution and size-resolved mixing state of aerosols in eastern China, CRIs of BC containing
55 and BC free aerosols were investigated separately based on Mie theory for sphere and core-shell structure, the corresponding CRIs were $1.67\pm 0.67i$ and 1.37-1.51. Wang et al. (2021) measured optical properties and size distribution of rural aerosol using a three-wavelength albedometer combined with a scanning mobility particle sizer (SMPS) and an APS, CRIs were obtained based on Mie theory by assuming aerosol as homogeneous spheres, and the fractions of preset four compositions were further clarified using volume mixing rule.

60 Experiment studies focus on the ambient aerosols, the inherent microphysical parameters such as morphology and mixing structures of typical black carbon and dust aerosols cannot be considered effectively, which can be explored through numerical simulation and theoretical analysis. To represent the morphological characteristics of mineral dust, Zong et al. (2021) developed the inhomogeneous super-spheroid model containing inside spheres, absorption, and scattering coefficients



were used to obtain CRIs at 0.2-1.0 μm wavelengths based on Lorenz-Mie theory for homogeneous spheres, they stressed
65 the adopted size distribution of spheres have significant effects on the CRIs. Furthermore, Kong et al. (2023) employed the
inhomogeneous super-spheroid model consisting of several separate mineral components to simulate dust aerosol, calculated
scattering and absorption coefficients were used to retrieve effective CRIs based on homogeneous super-spheroid and sphere
models, results showed that imaginary part of CRIs can be retrieved more credibly from absorption than the retrieval of both
real and imaginary part. Zhang et al. (2019b) employed polydisperse core-shell models to represent internal-mixed BC
70 aerosols coated by sulfate, scattering and absorption cross sections were calculated and used to further retrieve optically
effective CRIs based on single sphere Mie calculations, they revealed that the retrieved imaginary part of CRIs was
significantly lower than those approximated by VWA method by 3 times. Furthermore, Zhang et al. (2019a) developed
coated aggregates to represent aged BC aerosol, scattering and absorption properties were simulated using the multiple-
sphere T-matrix method (MSTM), optically effective CRIs were obtained through the Mie theory and compared with those
75 estimated by VWA method and effective medium theory (EMT), results showed that the shell/core ratio, geometry and size
distribution have complicated effects on the retrieved CRIs, VWA and EMT methods performed well in predict optical
effective CRIs for aerosols in accumulation mode, however, these two methods produce imaginary parts 2 times higher than
optical effective ones for coarse coated BC.

Most of the studies focusing on the optically effective CRIs from both experimental and numerical aspects were conducted
80 with the hypothesis that aerosols especially BC are homogeneous or at least the coatings were homogeneous, which is not in
line with the realistic aging process including condensation, photochemical reaction, and hygroscopic growth. The transition
from hydrophobic to hydrophilic is one of the uniqueness of BC aerosol after it is coated by inorganic salt or organics.
During the hygroscopic growth of coated BC, atmospheric water is absorbed into coatings, the original coating materials,
which are assumed to as liquid state in this study, will be diluted, the CRI of coatings will be changed gradually towards the
85 CRI of water. Furthermore, the size of coated BC particle will be enlarged. Therefore, the optical properties including
scattering and absorption change accordingly under the coupling effects of the altered lensing effect and the scattering of
diluted coatings, which brings additional large uncertainties in radiative effects of BC aerosols under high relative humidity
(RH).

On the other hand, if the variation of optically effective CRIs of BC coating materials at different RHs can be retrieved
90 exactly based on scattering and absorption properties, the water content in coatings can be further calculated based on
mixing rules, which is meaningful in understanding the water uptake speed of coating materials and even the heterogeneous
chemical reaction. To explore the possibility of acquiring water content in coatings from optical observations, the following
questions are focused on in this study:

- Which observation wavelength and optical property are better to be employed to retrieve CRIs of coatings?
- 95 -How do microphysical properties such as morphology, size distribution, and aging degree affect the retrieved CRIs?
- What is the performance of optically effective CRIs in water content calculation at different relative humidity?



Theoretical analyses from numerical aspects are illustrated to answer the above three questions. Three typical morphological models are employed to represent BC coated by non-absorptive sulfate at different aging statuses (thinly-coated, partially-coated, and heavily-coated BC) and six RH values in the range 0-95% are selected. Scattering coefficient, absorption coefficient, and single scattering albedo of morphologically realistic aged BC at 532 and 1064 nm are calculated numerically using the precise multi-sphere T-matrix method (MSTM). The optical equivalent CRIs of coatings at different RHs are retrieved based on Mie theory using optical properties of coated fractal BC as references, and the water content in coatings is calculated through the effective medium mixing rule.

2 Model and methodology

2.1 Models of coated BC

Freshly emitted bare black carbon particles are fractal clusters composed of many monomers, the fractal aggregates can be constructed using the DLA algorithm package based on the well-known scaling laws (Wozniak et al., 2012):

$$N = K_f \left(\frac{R_g}{a} \right)^{D_f}, \quad (1)$$

$$R_g^2 = \frac{1}{N} \sum_{i=1}^N r_i^2, \quad (2)$$

where a is monomer radius, N is monomer number, K_f is the fractal prefactor, D_f is the fractal dimension that controls the compactness of BC aggregate, R_g is gyration radius which describes the spatial size of the aggregate, r_i represents the distance between the i th monomer and the mass center of whole aggregate. These morphological parameters constrain the arrangement of each monomer in fractal aggregates. The optical especially absorption property is much less sensitive to K_f than that to D_f , thus K_f is set to constant 1.20, while D_f varies in the range of 1.80-2.80 (Amin et al., 2019). To facilitate the conversion of volume fraction, the black carbon monomer is assumed to be monodispersed and the radius is set to 20 nm (Wu et al., 2016; Yin and Liu, 2010). To ensure the size of fractal aggregate models covers most observations of black carbon, monomer number N ranges from 50 to 2000, and the maximum volume equivalent size reaches about 500 nm.

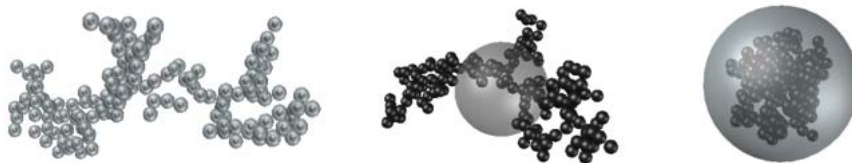
During the atmospheric aging process, bare black carbon is coated by materials like sulfate, resulting in inhomogeneous mixing structures (Kholghy, 2012). In this study, the coating material is assumed to be spherical. The volume fraction of BC (V_f) is taken to describe the mixing state of coated BC aerosols (Wu et al., 2014):

$$V_f = \frac{V_{BC}}{V_{total}}, \quad (3)$$

where V_{BC} and V_{total} represent the volume of black carbon and the whole coated particle, respectively. For a better representation of atmospheric black carbon aerosols at different aging states, the closed-cell model (CCM), partially-coated



125 model (PCM), and coated-aggregated model (CAM) are selected and investigated, as shown in Fig. 1. The V_f ranges from 1 to 0.05, the values of both V_f and D_f for different models is slightly different to related to aging states.



(a) CCM with $D_f=1.80$, $V_f=0.10$ (b) PCM $D_f=1.80$, $V_f=0.40$ (c) CAM with $D_f=2.60$, $V_f=0.10$

Figure 1: An example for accurate data representation & universal readability of figures.

2.2 Microphysical properties at different RHs

130 In this study, the bare black carbon particles are assumed to be coated by hydrophilic sulfate, and the optical properties at both 532 and 1064 nm wavelengths are investigated. Bond and Bergstrom (2006) demonstrated that the CRI of black carbon almost has no spectrum dependence within the visible and near-infrared wavelengths. The sulfate is considered to be non-absorptive, thus its imaginary part of CRI is always set to 0. CRIs of black carbon and sulfate employed are $2.26+1.26i$ and $1.50+0i$, respectively (Zhang et al., 2019c).

135 Under different relative humidities in atmosphere, sulfate coatings absorb moisture and thus change both the particle size of coated BC and CRIs of coatings (Mason et al., 2015). The CRIs of sulfate solutions during the hygroscopic process can be well described by the typical two-component effective medium theory Bruggeman approximation (Luo et al., 2018a):

$$f_s \frac{\epsilon_s - \epsilon}{\epsilon_s + 2\epsilon} + f_w \frac{\epsilon_w - \epsilon}{\epsilon_w + 2\epsilon} = 0, \quad (4)$$

$$m = \sqrt{\epsilon}, \quad (5)$$

140 where the volume fractions of sulfate and water satisfy $f_s+f_w=1$, ϵ_s and ϵ_w are the dielectric constants of sulfate and water respectively, m and ϵ are the effective refractive index and the effective dielectric constant for the coatings at different RHs. The variation of particle size during the hygroscopic growth of coated BC can be calculated according to the κ -Kohler theory (Zhao et al., 2022; Kuang et al., 2020):

$$RH = \frac{(D/D_i)^3 - 1}{(D/D_i)^3 - (1 - \kappa)} \exp\left(\frac{4\partial M_w}{\rho_w R T D}\right), \quad (6)$$

145 where D_i and D are the diameters of coated BC at dry and moist state respectively, ∂ is the surface tension of water droplet, M_w and ρ_w are the molar mass and density of water respectively, R is the universal gas constant, T is the temperature, and κ is the hygroscopic parameter which is selected as 0.52 (Liu et al., 2014).



2.3 Optical simulation and CRI retrieval

Many numerical simulation methods have been developed for the optical calculation of morphological complex BC models (Zhang et al., 2018). The multi-sphere T-matrix method (MSTM), which is developed based on T-matrix theory and employs the addition theorem of vector spherical wave functions to explain the interactions between different monomers in a multi-sphere system, is efficient and accurate among all these methods (Mackowski, 2014). MSTM is suitable for sphere clusters with any morphology that contact in inside or outside form, but the limitation is that the spheres cannot overlap with each other (Mackowski and Mishchenko, 1996). With the input of CRIs for BC and coatings as well as the center coordinates and radii of spheres, the optical properties such as optical efficiency (Q), optical cross section (C), single scattering albedo (SSA) and so on for coated BC aerosol could be exactly simulated (He et al., 2015).

Aerosol scattering and absorption properties are directly related to the real and imaginary parts of CRIs respectively, thus these two parameters are commonly used for the retrieval of CRIs in laboratory and field observations (Virkkula et al., 2006). Since SSA is the ratio of scattering to extinction (sum of scattering and absorption), the performance of SSA in CRIs retrieval is examined in this study. For the optical retrieval of CRIs for coated BC, firstly, the microphysical parameters such as volume equivalent diameter of whole particle and effective CRIs of coatings under different RHs are calculated. Then, the optical properties of complex coated BC during the hygroscopic growth process are optically simulated using MSTM. Optical property look-up tables of core-shell models are constructed based on Mie theory with real part and imaginary part of CRIs ranging from 1.00-1.80 and 0-0.20 respectively. Finally, the optical equivalent CRIs of coated BC at different RHs and wavelengths are retrieved through minimum distinctions of selected optical properties between fractal model and core-shell model with the same particle size. The objective function employed for optical retrieval is as follows:

$$\chi^2 = \left(\frac{\sigma_{sca,MSTM}(n,k) - \sigma_{sca,Mie}(n,k)}{\sigma_{sca,MSTM}(n,k)} \right)^2 + \left(\frac{\sigma_{abs,MSTM}(n,k) - \sigma_{abs,Mie}(n,k)}{\sigma_{abs,MSTM}(n,k)} \right)^2 + \left(\frac{SSA_{MSTM}(n,k) - SSA_{Mie}(n,k)}{SSA_{MSTM}(n,k)} \right)^2, \quad (7)$$

where σ is the optical properties, the subscript *sca* and *abs* are the scattering and absorption respectively, and the MSTM and Mie represent the optical properties for coated aggregate model and core-shell model.

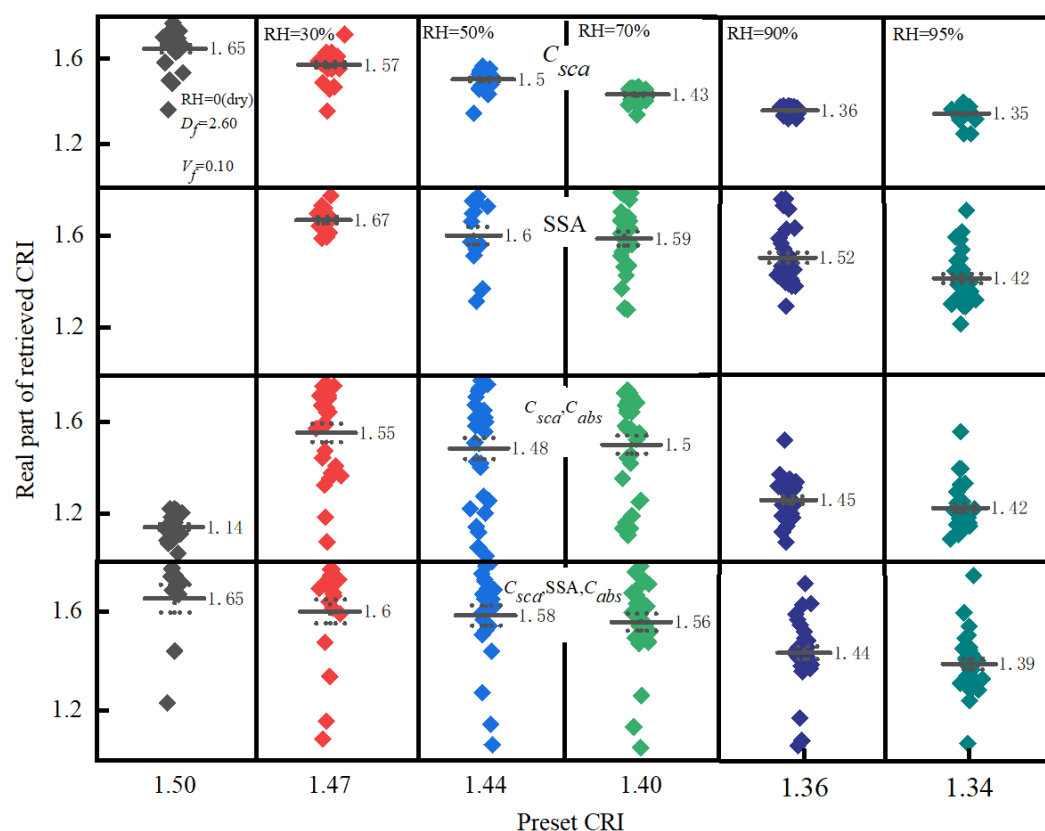
3. Result and discussion

3.1 Performance of optical properties at different wavelengths

The optical properties for fractal BC models and core-shell models are distinct evidently to varying degrees, in some cases, the evolution of optical properties with both the real part and imaginary part of CRIs for these two models even cannot overlap, indicating that the CRI for coated BC would not be retrieved. Moreover, the retrieved real parts of CRIs can be larger than 1.50 or smaller than 1.33, and the retrieved imaginary parts of CRIs can be non-vanishing, which means that the retrieved results are physically meaningless. Fig. 2. describes the retrieved real part of CRIs of coated-aggregate models with



180 $D_f=2.60$ and $V_f=0.10$ at different RHs, different combinations of scattering cross section (C_{sca}), absorption cross section (C_{abs}), and single scattering albedo (SSA) are selected for the CRI retrieval. The horizontal solid line and the vertical dotted line represent the mean value and the error respectively. It can be seen that the C_{sca} has the best performance among all these optical parameters, the mean value of retrieved real part of CRIs is the closest to the preset values of coatings, the deviation is smaller and the results are more concentrated on the mean values. However, the retrieved results for other optical properties and their combinations are more dispersed and fluctuated. The retrieved data would diminish at low humidity, there would even be no data when SSA is employed at RH=0. Therefore, only the scattering cross section is selected for further investigation on the retrieved CRIs and water contents in coatings.



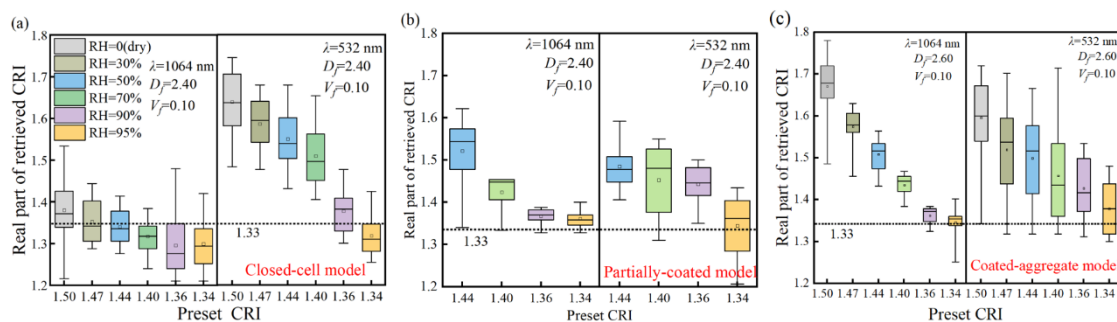
185

Figure 2. Comparison of preset and retrieved real parts of CRIs based on different optical properties of coated-aggregate BC models with $D_f=2.60$ and $V_f=0.10$ at different RHs.

190 Figure 3. illustrates the retrieved real part of CRIs of coated BC with closed-cell, partially-coated, and coated-aggregate models with $V_f=0.10$ at different RHs and wavelengths. Two typical wavelengths at visible (532 nm) and near-infrared (1064 nm) spectrum are considered. The bottom and top of the boxes represent the 25th and 75th percentiles respectively, the short lines and dots inside the boxes represent the median and mean values respectively, and the upper and lower whiskers represent the maximum and minimum values respectively. When the atmospheric relative humidity increases from 0 to 95%,



the effective real part of CRIs for coatings after water absorption decrease gradually. The retrieved CRIs also decreases with the RHs for different morphological models at both 532 and 1064 nm. For closed-cell model, as shown in Fig. 3(a), the retrieved CRIs at two wavelengths are underestimated under all RHs, the relative errors in retrieved values increase with RHs at 532 nm while decreasing at 1064 nm, the overall performance at 532 nm is better than that at 1064 nm, and the largest relative error at RH=95% could be about 9.48%. For both partially-coated and coated-aggregate models, the retrieved CRIs are overestimated during the hygroscopic process of sulfate coatings. The averaged real parts of retrieved CRIs have an obvious deviation from the preset values when the relative humidity is small, but the deviations decrease and the retrieved values are closer to the preset values with the increase of RHs, averaged relative errors for coated-aggregate with $D_f = 2.60$ and $V_f = 0.10$ decrease from 8.06% to 5.38% at 532 nm, while decrease from 8.41% to 1.53% at 1064 nm. Compared with visible wavelength, the retrieval performances at 1064 nm are much better, the distributions of retrieval results are more centralized and stable.



205 **Figure 3. Comparison of preset and retrieved real part of CRIs of coated BC aerosols at different RHs and wavelengths. (a) Closed-cell model; (b) Partially-coated model; (c) Coated-aggregate model.**

3.2 Influence of microphysical parameter on the retrieved CRIs

Figure 4. describes the variation of retrieved real parts of CRIs of coated-aggregate models with different BC core sizes, BC volume fractions and fractal dimensions. With the increase of particle size, the retrieved results present typical arched distribution patterns, the retrieved real parts of CRIs increase at first and then decrease, the maximum can be reached when BC core sizes are in the range of about 160-180 nm. The effects of relative humidity on CRI retrieval are evident, the arched patterns turn to slight and the fitting goodness become much better at high RHs, the retrieved real parts of CRIs are more sensitive to size distribution at low RHs. With the increase of RHs, the averaged retrieval errors decrease from 6.77% to 1.09% for BC aerosol with $D_f = 2.80$ and $V_f = 0.10$. As shown in Fig. 4(b) and 4(d), the retrieved real parts of CRIs are smaller for larger BC cores with larger fractal dimensions. Furthermore, when BC volume fraction decrease from 0.10 to 0.075, the retrieved CRIs also decrease obviously.

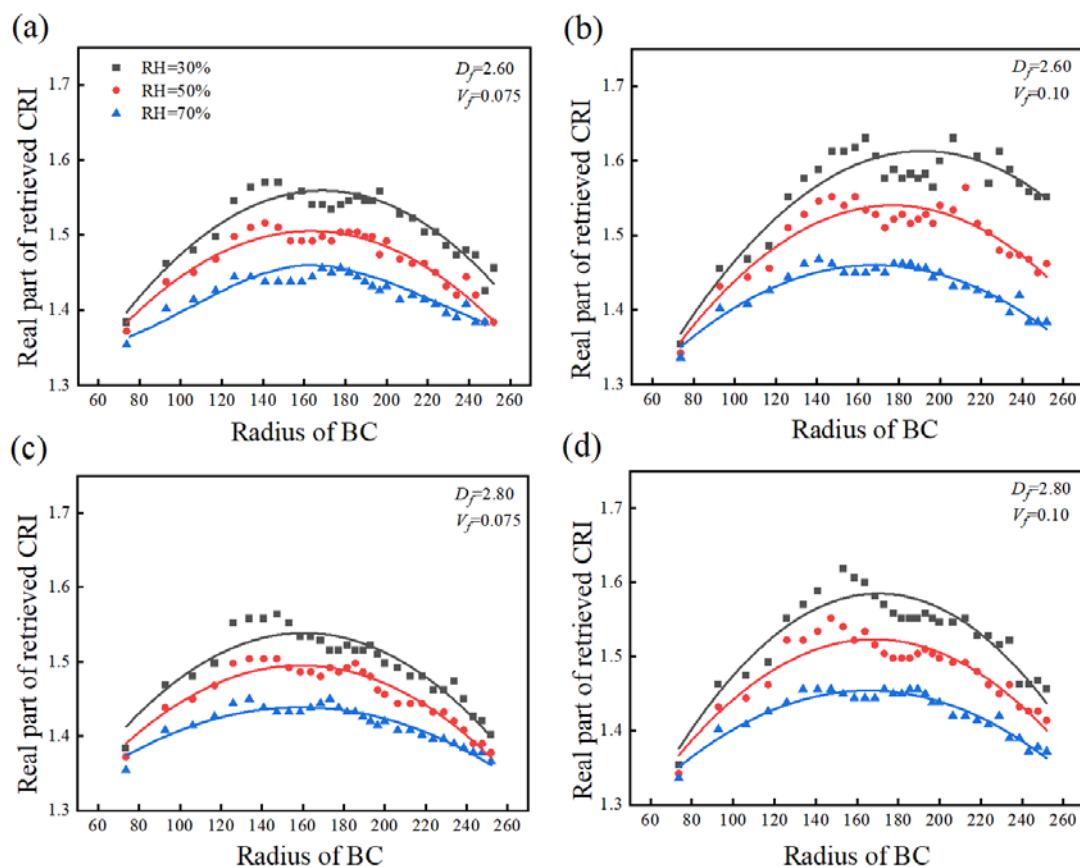


Figure 4. Retrieved real parts of CRIs of coated-aggregate models with different fractal dimensions and BC volume fractions during the hygroscopic process. (Retrieved results are shown in points and fitted in lines)

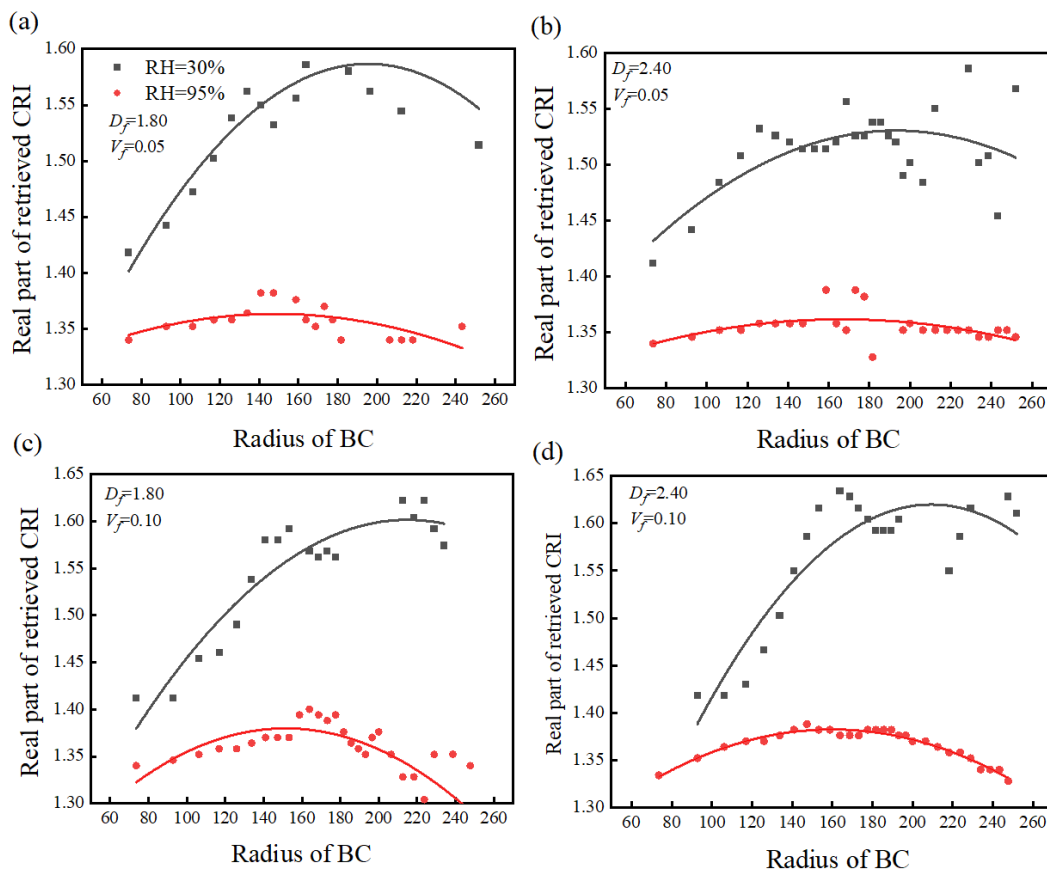
220 Figure 5. shows the variation of retrieved real parts of CRIs of partially-coated models at different RHs. Similar to coated-aggregate modes, the retrieved real parts of CRIs also increase at first and then decrease, but the maximum values are significantly affected by relative humidity. At high RHs, the sensitivity and fluctuation of CRIs with particle size are more inconspicuous. The averaged retrieval errors decrease from 4.87% to 1.51% for BC aerosol with $D_f=2.40$ and $V_f=0.05$ under different RHs. With the BC volume fraction V_f enlarged from 0.05 to 0.10, the retrieved results also increased slightly. Fig. 6.

225 shows the variation of retrieved real parts of CRIs of closed-cell models at different RHs. The retrieved results of CRIs increase with BC core radius in most cases, however, for particles with $D_f=1.80$ at dry state, the retrieved real parts of CRIs decrease at first and increase then. When RH increase from 0 to 95%, the optical equivalent real parts of CRIs decrease (Cotterell et al., 2017). During the hygroscopic growth, the mean retrieval errors decrease from 11.7% to 5.43% when the BC volume fraction and fractal dimension are 0.10 and 2.40 respectively. The retrieved refractive index would be enlarged

230 and more close to the preset values. It should be noted that some of the retrieved real parts of CRIs of closed-cell



models are smaller than 1.33, which is the CRI of water.(Virkkula et al., 2006) also proposed that the non-spherical morphology would lead to unreasonably low and meaningless values of effective aerosol refractive indices.



235 **Figure 5. Retrieved real parts of CRIs of partially-coated models with different fractal dimensions and BC volume fractions during the hygroscopic process. (Retrieved results are shown in points and fitted in lines)**

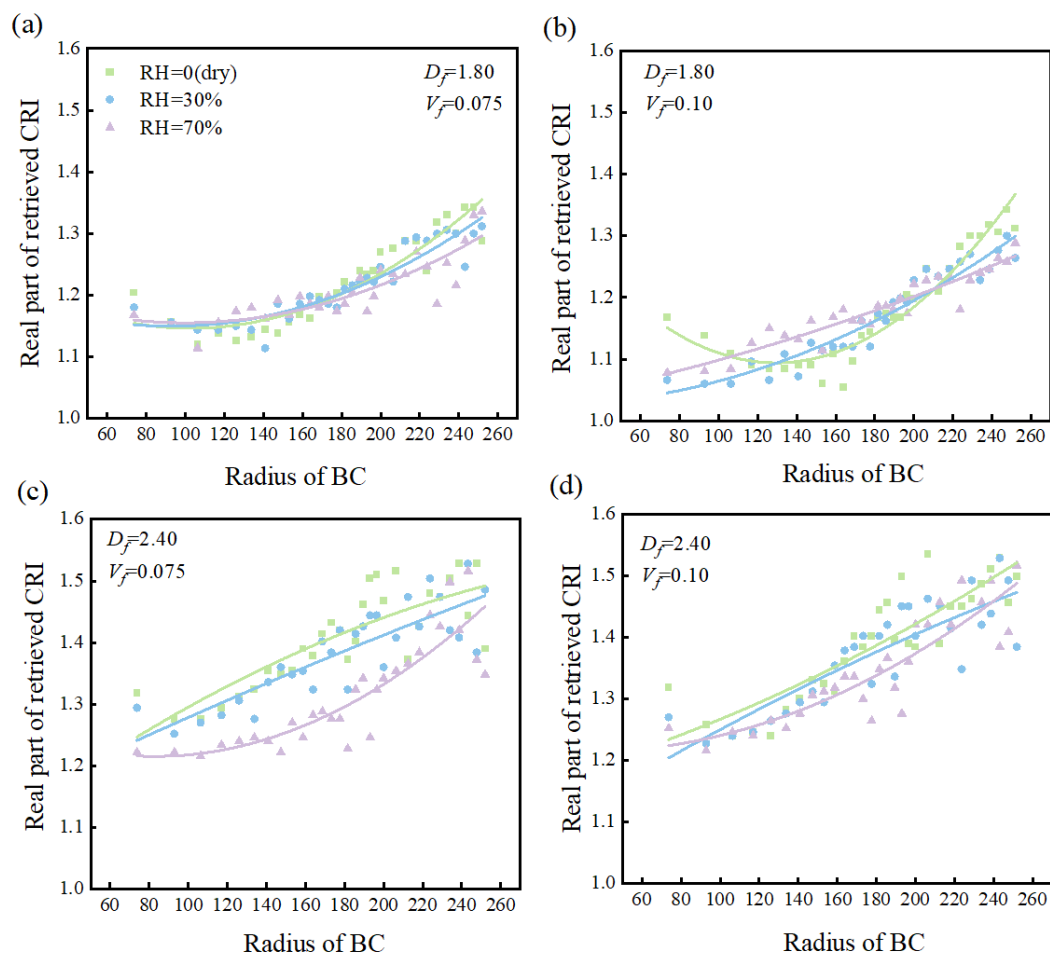


Figure 6. Retrieved real parts of CRIs of closed-cell model with different fractal dimensions and BC volume fractions during the hygroscopic process. (Retrieved results are shown in points and fitted in lines)

Figure 7. illustrates the comparisons of real parts of optical retrieved CRIs and the corresponding preset values during the hygroscopic process, all coated particles with different fractal dimensions, BC volume fractions, and BC core sizes are considered. The white dots in each violin plot represent the median value of retrieved real part, the areas are the probability distributions of all the data, the wider parts mean that the data is more concentrated. The optical retrieval performance is better for coated-aggregate and partially-coated models than that for closed-cell model, especially when RHs are larger than 70%. The enhanced aggregate compactness would facilitate the exact retrieval of CRIs at different RHs, the averaged retrieval error for coated-aggregate with $D_f=2.80$ could be reduced to about 6%, due to the similarity of coated-aggregate model and the core-shell model used for optical retrieval. The BC volume fractions also have some influences on the retrieval accuracy of CRIs, the retrieval errors are negligible for $V_f=0.05$ under 95% high humidity. Especially, the mean retrieval errors of CRIs for closed-cell model, partially-coated model, and coated-aggregate model reach 5.43%, 1.51%, and



1.09% respectively. With the increase of atmosphere humidity, the retrieval results are more and more reasonable, a larger amount of real part values range in 1.33-1.50, which are the refractive indices of water and sulfate respectively. When RHs are smaller than 30%, most of the retrieved real parts of CRIs for partially-coated and coated-aggregate model are larger than 1.50. Furthermore, the vast majority of the retrieval results (>75%) for closed-cell models are smaller than 1.33. More specifically, closed-cell models with compact structures ($D_f > 2.40$) performs better CRI retrieval than those with looser structures ($D_f < 1.80$), however, the retrieved data of the former is fewer. The fractal aggregate of BC and the non-spherical morphology of coated particles after moisture absorption leads to meaningless real parts under different RHs.

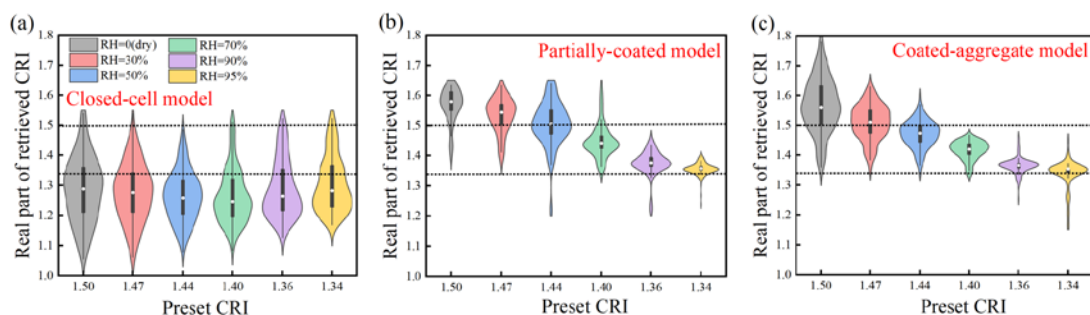


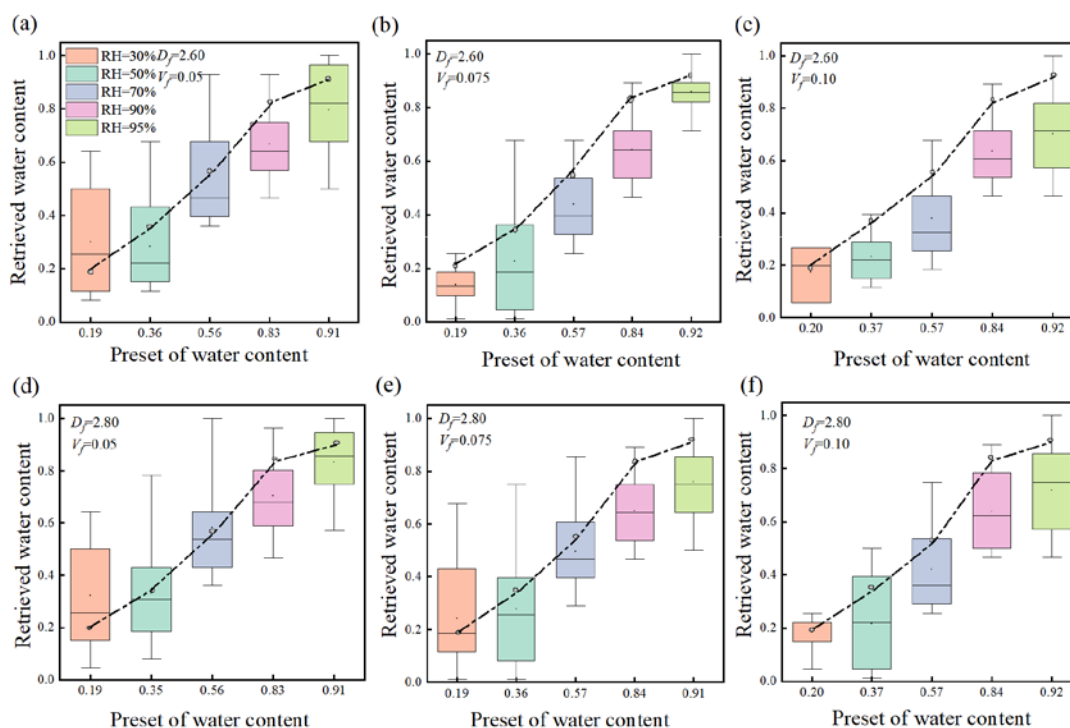
Figure 7. Retrieved refractive indices of closed-cell model, partially-coated model, and coated-aggregate model under different RHs.

3.3 Retrieval water content in coatings from CRIs

260 The effective medium theory can deal well with the dielectric constant and refractive index of homogeneous mixtures of different species. Bruggeman approximation, among all the effective medium theories, is suitable for the mixture of soluble sulfate and water. Based on the retrieved optical equivalent refractive index, the water contents at different RHs can be calculated. Fig.8. shows the comparisons of retrieved and preset water content in coatings for coated-aggregate models at different relative humidities. With RHs increasing from 30% to 95%, the retrieved water contents gradually increase, due to the enhanced water absorbing capacity. Fig. 8. (a-c) illustrates results for heavily aged coated-aggregate models with the same fractal dimension, when BC volume fractions decrease from 0.10 to 0.05, the retrieved water contents are closer to preset values under RHs larger than 50%, as can be seen from the 1:1 dividing lines in each subplot, and the retrieval is more accurate. However, under a low RH 30%, retrieval errors are enlarged with the decrease of V_f , and the averaged error is 62.68%. When V_f is small, the proportion of coatings is large, therefore the retrieved water content will be more reliable. As 270 can be seen from Fig. 8(c) and Fig. 8(f), the retrieved water contents of coated particles with larger fractal dimensions are more accurate than those with smaller D_f . For coated-aggregate models with large fractal dimension (2.80) and small BC volume fraction (0.05), the minimum value of retrieval errors can be about 2%. In addition, it should be noted that since the retrieved real part of CRIs can vary from 1.18 to 1.71, which are wider than the physically effective range 1.33-1.50, indicating that water contents for some coated BC particles cannot be obtained. Fig.9. illustrates the retrieved and preset



275 water content in coatings for partially-coated models at different RHs. Three RHs (70%, 90%, and 95%) are considered for
 partially-coated models with $D_f=1.80$, while four RHs (50%, 70%, 90%, and 95%) are considered for the same models with
 $D_f=2.40$, the reason is that even through optical equivalent CRIs could be retrieved under relatively low RHs but the
 retrieved results are smaller than CRI of water or larger than CRI of sulfate. The obtained water contents for partially-coated
 models are analogous to that for coated-aggregate models, relative errors are reduced with the increase of coating amount.
 280 Nevertheless, there are more retrieved abnormal results of CRIs smaller than 1.33, and water in coatings cannot be calculated.
 On the other hand, the normal looking results of CRIs have large deviations from the preset corresponding values, which
 further result in extreme water contents. In short, the water content retrieval for BC aerosols with thick coatings, that is in a
 severe aging state, have the best performance.



285 **Figure 8. Retrieved water content in coatings for coated-aggregate models with different D_f and V_f during the hygroscopic growth. The dotted lines are the 1:1 dividing lines.**

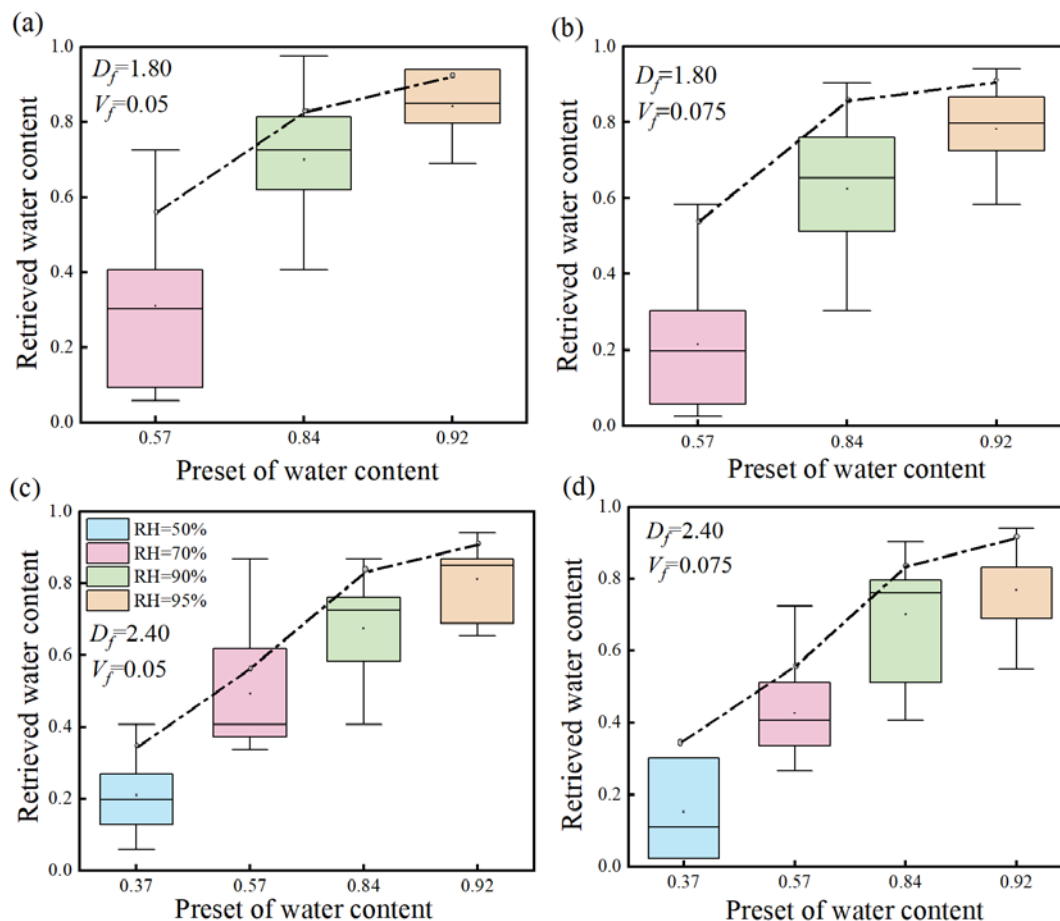


Figure 9. Retrieved water content in coatings for partially-coated models with different D_f and V_f during the hygroscopic growth. The dotted lines are the 1:1 dividing lines.

290 4. Conclusion

Black carbon (BC) aerosols coated with hydrophilic materials will absorb moisture at humid environments, the quantification of water content in the coatings of BC is significant for the investigation of heterogeneous reaction and hygroscopic growth. In this study, a method to obtain water content is investigated based on the complex refractive index retrieved using optical properties. From numerical inspections, optical properties of coated BC aerosols under six RHs from 0 to 295 95% at both 532 and 1064 nm are simulated with the assistance of three realistic fractal models: closed-cell model, partially-coated model and coated-aggregate model. The optical equivalent complex radiative indices (CRIs) of coatings are retrieved based on core-shell Mie theory, furthermore, the water contents in coatings at different RHs are investigated theoretically through effective medium theory.



Scattering properties, among all the optical parameters and their combinations, have the best performance in retrieving CRIs
of coatings of aged BC. With the RHs increase from 0 to 90%, the retrieved CRIs for closed-cell models are underestimated
at both 532 and 1064 nm, and the retrieved CRIs for both partially-coated and coated-aggregate models are overestimated.
The averaged relative errors for coated-aggregate models with $D_f=2.60$ and $V_f=0.10$ range from 5.38% to 8.06% at 532 nm,
while relative errors range from 1.53% to 8.41% at 1064 nm. Generally, the CRI retrieval performance at 1064 nm
wavelength is better. The retrieved real part of CRIs for all these three models decreases with the increased RHs, and
retrieval errors also decrease. The retrieval accuracy of CRIs for coated-aggregate models are better than other two fractal
models. When the RH reaches 95%, the minimum retrieval errors for closed-cell, partially-coated and coated-aggregate
models are 5.43%, 1.51%, and 1.09% respectively. Fractal BC models with compact structures and small BC volume
fractions performs well in the CRI retrieval. However, in certain situations such as closed-cell model with $D_f=1.80$ and
 $V_f=0.10$, the retrieved real part of CRIs under low humidities are meaningless, which are smaller than that of water (1.33) or
larger than that of sulfate (1.50).

The water contents in the coatings of aged BC aerosols at different RHs can be effectively calculated from the optical
equivalent CRIs of coatings based on Bruggeman's approximation effective medium theory. The retrieved water contents
gradually increase when RHs range in 30-95%. The water content retrieval for fractal BC aerosols with smaller BC volume
fractions and larger fractal dimensions are more accurate. For severely aged coated-fractal BC aerosol, the retrieval errors of
water contents are the smallest, which are 2%-63%. Nevertheless, the complex morphologies of coated BC aerosols could
result in unreasonable CRIs of coatings and further cause missed results of water content. This study constructs a useful
method to obtain refractive index and water content of BC coatings during the hygroscopic growth process, and also
highlights the possible retrieval errors caused by non-sphericity of BC aerosols when the famous core-shell Mie theory is
employed for the optical retrieval.

320

Author contribution. LJ and ZC planned the campaign; ZC and ZD performed the investigation and data analysis; ZC
wrote the manuscript draft; LJ and HJ reviewed and edited the manuscript.

325 **Fundings.** This research has been supported by the National Natural Science Foundation of China (grant no. 42305082,
U23A20678), the Science Research Project of Hebei Education Department (grant no. BJK2024179), and the Innovation
Team of Nondestructive Testing Technology and Instrument, Hebei University (IT2023C03)

330 **Acknowledgments.** We particularly thank Dr. Mishchenko M. I. and Dr. Mackowski D. W. for the MSTM code. We also
appreciate the support of the supercomputing center of Hebei University.

Disclosures. The authors declare no conflicts of interest relevant to this study.



Data availability. Processed data for this study are available online (<https://doi.org/10.13140/RG.2.2.21765.36321>).

335

References

- Amin, H. M. F., Bennett, A., and Roberts, W. L.: Determining fractal properties of soot aggregates and primary particle size distribution in counterflow flames up to 10 atm, *Proc. Combust. Inst.*, 37, 1161-1168, [10.1016/j.proci.2018.07.057](https://doi.org/10.1016/j.proci.2018.07.057), 2019.
- Bond, T. C. and Bergstrom, R. W.: Light absorption by carbonaceous particles: An investigative review, *Aerosol Sci. Technol.*, 40, 27-67, [10.1080/02786820500421521](https://doi.org/10.1080/02786820500421521), 2006.
- 340 Cotterell, M. I., Willoughby, R. E., Bzdek, B. R., Orr-Ewing, A. J., and Reid, J. P.: A complete parameterisation of the relative humidity and wavelength dependence of the refractive index of hygroscopic inorganic aerosol particles, *Atmos. Chem. Phys.*, 17, 9837-9851, [10.5194/acp-17-9837-2017](https://doi.org/10.5194/acp-17-9837-2017), 2017.
- He, C., Liou, K. N., Takano, Y., Zhang, R., Zamora, M. L., Yang, P., Li, Q., and Leung, L. R.: Variation of the radiative properties during black carbon aging: theoretical and experimental intercomparison, *Atmos. Chem. Phys.*, 15, 11967-11980, [10.5194/acp-15-11967-2015](https://doi.org/10.5194/acp-15-11967-2015), 2015.
- 345 He, Q. F., Bluvshstein, N., Segev, L., Meidan, D., Flores, J. M., Brown, S. S., Brune, W., and Rudich, Y.: Evolution of the Complex Refractive Index of Secondary Organic Aerosols during Atmospheric Aging, *Environ. Sci. Technol.*, 52, 3456-3465, [10.1021/acs.est.7b05742](https://doi.org/10.1021/acs.est.7b05742), 2018.
- 350 Kholghy, M. R.: The Evolution of Soot Morphology in Laminar Co-Flow Diffusion Flames of the Surrogates for Jet A-1 and a Synthetic Kerosene, 2012.
- Kong, S., Wang, Z., and Bi, L.: The uncertainties in the laboratory-measured short-wave refractive indices of mineral dust aerosols and the derived optical properties: A theoretical assessment, *EGUsphere*, 2023, 1-36, 2023.
- Kuang, Y., Xu, W. Y., Tao, J. C., Ma, N., Zhao, C. S., and Shao, M.: A Review on Laboratory Studies and Field Measurements of Atmospheric Organic Aerosol Hygroscopicity and Its Parameterization Based on Oxidation Levels, *Curr. Pollut. Rep.*, 6, 410-424, [10.1007/s40726-020-00164-2](https://doi.org/10.1007/s40726-020-00164-2), 2020.
- 355 Liu, H. J., Zhao, C. S., Nekat, B., Ma, N., Wiedensohler, A., van Pinxteren, D., Spindler, G., Müller, K., and Herrmann, H.: Aerosol hygroscopicity derived from size-segregated chemical composition and its parameterization in the North China Plain, *Atmos. Chem. Phys.*, 14, 2525-2539, [10.5194/acp-14-2525-2014](https://doi.org/10.5194/acp-14-2525-2014), 2014.
- 360 Luo, J., Zhang, Y. M., and Zhang, Q. X.: A model study of aggregates composed of spherical soot monomers with an acentric carbon shell, *J. Quant. Spectrosc. Radiat. Transf.*, 205, 184-195, [10.1016/j.jqsrt.2017.10.024](https://doi.org/10.1016/j.jqsrt.2017.10.024), 2018a.
- Luo, J., Zhang, Y. M., Wang, F., and Zhang, Q. X.: Effects of brown coatings on the absorption enhancement of black carbon: a numerical investigation, *Atmos. Chem. Phys.*, 18, 16897-16914, [10.5194/acp-18-16897-2018](https://doi.org/10.5194/acp-18-16897-2018), 2018b.



- Mackowski, D. W.: A general superposition solution for electromagnetic scattering by multiple spherical domains of optically active media, *J. Quant. Spectrosc. Radiat. Transf.*, 133, 264-270, 10.1016/j.jqsrt.2013.08.012, 2014.
- Mackowski, D. W. and Mishchenko, M. I.: Calculation of the T matrix and the scattering matrix for ensembles of spheres, *J. Opt. Soc. Am. A*, 13, 2266-2278, 10.1364/JOSAA.13.002266, 1996.
- Mason, B. J., Cotterell, M. I., Preston, T. C., Orr-Ewing, A. J., and Reid, J. P.: Direct Measurements of the Optical Cross Sections and Refractive Indices of Individual Volatile and Hygroscopic Aerosol Particles, *J. Phys. Chem. A*, 119, 5701-5713, 10.1021/acs.jpca.5b00435, 2015.
- Radney, J. G. and Zangmeister, C. D.: Comparing aerosol refractive indices retrieved from full distribution and size- and mass-selected measurements, *J. Quant. Spectrosc. Radiat. Transf.*, 220, 52-66, 10.1016/j.jqsrt.2018.08.021, 2018.
- Virkkula, A., Koponen, I. K., Teinilä, K., Hillamo, R., Kerminen, V. M., and Kulmala, M.: Effective real refractive index of dry aerosols in the Antarctic boundary layer, *Geophys. Res. Lett.*, 33, 4, 10.1029/2005gl024602, 2006.
- Wang, S., Crumeyrolle, S., Zhao, W. X., Xu, X. Z., Fang, B., Derimian, Y., Chen, C., Chen, W. D., Zhang, W. J., Huang, Y., Deng, X. L., and Tong, Y. X.: Real-time retrieval of aerosol chemical composition using effective density and the imaginary part of complex refractive index, *Atmos. Environ.*, 245, 14, 10.1016/j.atmosenv.2020.117959, 2021.
- Wozniak, M., Onofri, F. R. A., Barbosa, S., Yon, J., and Mroczka, J.: Comparison of methods to derive morphological parameters of multi-fractal samples of particle aggregates from TEM images, *J. Aerosol. Sci.*, 47, 12-26, 10.1016/j.jaerosci.2011.12.008, 2012.
- Wu, Y., Cheng, T. H., Zheng, L. J., and Chen, H.: Models for the optical simulations of fractal aggregated soot particles thinly coated with non-absorbing aerosols, *J. Quant. Spectrosc. Radiat. Transf.*, 182, 1-11, 10.1016/j.jqsrt.2016.05.011, 2016.
- Wu, Y., Cheng, T. H., Gu, X. F., Zheng, L. J., Chen, H., and Xu, H.: The single scattering properties of soot aggregates with concentric core-shell spherical monomers, *J. Quant. Spectrosc. Radiat. Transf.*, 135, 9-19, 10.1016/j.jqsrt.2013.11.009, 2014.
- Xu, X. Z., Zhao, W. X., Zhang, Q. L., Wang, S., Fang, B., Chen, W. D., Venables, D. S., Wang, X. F., Pu, W., Wang, X., Gao, X. M., and Zhang, W. J.: Optical properties of atmospheric fine particles near Beijing during the HOPE-J3A campaign, *Atmos. Chem. Phys.*, 16, 6421-6439, 10.5194/acp-16-6421-2016, 2016.
- Xu, X. Z., Zhao, W. X., Qian, X. D., Wang, S., Fang, B., Zhang, Q. L., Zhang, W. J., Venables, D. S., Chen, W. D., Huang, Y., Deng, X. L., Wu, B. W., Lin, X. F., Zhao, S., and Tong, Y. X.: The influence of photochemical aging on light absorption of atmospheric black carbon and aerosol single-scattering albedo, *Atmos. Chem. Phys.*, 18, 16829-16844, 10.5194/acp-18-16829-2018, 2018.
- Yin, J. Y. and Liu, L. H.: Influence of complex component and particle polydispersity on radiative properties of soot aggregate in atmosphere, *J. Quant. Spectrosc. Radiat. Transf.*, 111, 2115-2126, 10.1016/j.jqsrt.2010.05.016, 2010.
- Zhang, X. L., Mao, M., and Chen, H. B.: Characterization of optically effective complex refractive index of black carbon composite aerosols, *J. Atmos. Sol.-Terr. Phys.*, 198, 8, 10.1016/j.jastp.2019.105180, 2020.
- Zhang, X. L., Mao, M., and Yin, Y.: Optically effective complex refractive index of coated black carbon aerosols: from numerical aspects, *Atmos. Chem. Phys.*, 19, 7507-7518, 10.5194/acp-19-7507-2019, 2019a.



- Zhang, X. L., Jiang, H., Mao, M., and Yin, Y.: Does optically effective complex refractive index of internal-mixed aerosols have a physically-based meaning?, *Opt. Express*, 27, A1216-A1224, 10.1364/oe.27.0a1216, 2019b.
- 400 Zhang, X. L., Mao, M., Yin, Y., and Wang, B.: Numerical Investigation on Absorption Enhancement of Black Carbon Aerosols Partially Coated With Nonabsorbing Organics, *J. Geophys. Res.-Atmos.*, 123, 1297-1308, 10.1002/2017jd027833, 2018.
- Zhang, Y. X., Li, M., Cheng, Y. F., Geng, G. N., Hong, C. P., Li, H. Y., Li, X., Tong, D., Wu, N. N., Zhang, X., Zheng, B., Zheng, Y. X., Bo, Y., Su, H., and Zhang, Q.: Modeling the aging process of black carbon during atmospheric transport using a new approach: a case study in Beijing, *Atmos. Chem. Phys.*, 19, 9663-9680, 10.5194/acp-19-9663-2019, 2019c.
- 405 Zhao, G., Li, F., and Zhao, C. S.: Determination of the refractive index of ambient aerosols, *Atmos. Environ.*, 240, 9, 10.1016/j.atmosenv.2020.117800, 2020.
- Zhao, G., Tan, T. Y., Zhao, W. L., Guo, S., Tian, P., and Zhao, C. S.: A new parameterization scheme for the real part of the ambient urban aerosol refractive index, *Atmos. Chem. Phys.*, 19, 12875-12885, 10.5194/acp-19-12875-2019, 2019.
- 410 Zhao, G., Hu, M., Fang, X., Tan, T. Y., Xiao, Y., Du, Z. F., Zheng, J., Shang, D. J., Wu, Z. J., Guo, S., and Zhao, C. S.: Larger than expected variation range in the real part of the refractive index for ambient aerosols in China, *Sci. Total Environ.*, 779, 9, 10.1016/j.scitotenv.2021.146443, 2021.
- Zhao, P. S., Ge, S. S., Su, J., Ding, J., and Kuang, Y.: Relative Humidity Dependence of Hygroscopicity Parameter of Ambient Aerosols, *J. Geophys. Res.-Atmos.*, 127, 10, 10.1029/2021jd035647, 2022.
- 415 Zhao, W., Xu, X., Dong, M., Chen, W., Gu, X., Hu, C., Huang, Y., Gao, X., Huang, W., and Zhang, W.: Development of a cavity-enhanced aerosol albedometer, *Atmos. Meas. Tech.*, 7, 2551-2566, 10.5194/amt-7-2551-2014, 2014.
- Zong, R., Weng, F., Bi, L., Lin, X., Rao, C., and Li, W.: Impact of hematite on dust absorption at wavelengths ranging from 0.2 to 1.0 μm : an evaluation of literature data using the T-matrix method, *Opt. Express*, 29, 17405-17427, 2021.